

## Se<sub>2</sub>Mo<sub>10</sub>V<sub>3</sub>, a heteropoly compound containing selenium, inhibits tumor growth

Hong-Ning Zhang<sup>1</sup>, Wei-Li Feng<sup>2</sup>, Chun-Na An<sup>3</sup> and Wen-Guang Li<sup>4</sup>

<sup>1</sup>Department of Pharmacology, School of Basic Medical Sciences, Capital Medical University, Beijing 100069, China

<sup>2</sup>Department of Pharmacology, School of Basic Medical Sciences, Qinghai University, Xining 810001, China

<sup>3</sup>Department of Pharmacology, School of Basic Medical Sciences, North China University of Science and Technology, Tangshan 063009, China

<sup>4</sup>Department of Pharmacology, School of Basic Medical Sciences, Lanzhou University, Lanzhou 730000, China

**Correspondence to:** Chun-Na An, **email:** ancna@126.com  
Wen-Guang Li, **email:** zhangxz2012@yeah.net

**Keywords:** heteropoly compound containing selenium, Se<sub>2</sub>Mo<sub>10</sub>V<sub>3</sub>, anti-tumor, apoptosis, NF-κB/IκBα

**Received:** March 21, 2017

**Accepted:** May 30, 2017

**Published:** July 01, 2017

**Copyright:** Zhang et al. This is an open-access article distributed under the terms of the Creative Commons Attribution License 3.0 (CC BY 3.0), which permits unrestricted use, distribution, and reproduction in any medium, provided the original author and source are credited.

### ABSTRACT

**Selenium compounds have strong anti-tumor effects and are well-tolerated. We examined the anti-tumor effects of (NH<sub>4</sub>)<sub>2</sub>H<sub>15</sub>Se<sub>2</sub><sup>VI</sup>Mo<sub>10</sub>V<sub>3</sub>O<sub>52</sub>·2H<sub>2</sub>O (Se<sub>2</sub>Mo<sub>10</sub>V<sub>3</sub>), a heteropoly compound containing selenium. Se<sub>2</sub>Mo<sub>10</sub>V<sub>3</sub> inhibited proliferation in K562 cells with a half-maximal inhibitory concentration of 78.72±2.82 mg/L after 48 h and 24.94±0.88 mg/L after 72 h. Typical apoptotic morphologies were also observed in K562 cells treated with Se<sub>2</sub>Mo<sub>10</sub>V<sub>3</sub>, as were increased intracellular levels of Ca<sup>2+</sup>, Mg<sup>2+</sup>, H<sup>+</sup>, and reactive oxygen species, and decreased mitochondrial membrane potential. In addition, Se<sub>2</sub>Mo<sub>10</sub>V<sub>3</sub> treatment triggered cytochrome C release and inhibited IκBα degradation and NF-κB translocation. *In vivo* experiments revealed that 5 or 10 mg/kg Se<sub>2</sub>Mo<sub>10</sub>V<sub>3</sub> inhibited the growth of sarcoma 180 and hepatoma 22 xenograft tumors. These results indicate that Se<sub>2</sub>Mo<sub>10</sub>V<sub>3</sub> inhibits tumor growth both *in vitro* and *in vivo* and induces apoptosis in K562 cells, possibly by inhibiting the NF-κB/IκBα pathway.**

### INTRODUCTION

Selenium, an essential non-metal trace element [1], is crucial to the function of several enzymes, including glutathioneperoxidases and thioredoxin reductases [2]. Selenium deficiency is related to tumorigenesis, and selenium recruitment reduces the risk of cancer in humans [3, 4]. Furthermore, selenium compounds can prevent tumor formation [5], mainly by inducing apoptosis [6]. For example, Yang and Wang found that Na<sub>5</sub>SeV<sub>5</sub>O<sub>18</sub>·H<sub>20</sub>, a heteropoly compound containing selenium, had anti-tumor effects both *in vitro* and *in vivo* [7]. When used as therapeutic agents in tumor patients, selenium compounds are well-tolerated [8].

The possible anti-tumor effects and related underlying mechanisms for another selenium-containing heteropoly compound, (NH<sub>4</sub>)<sub>2</sub>H<sub>15</sub>Se<sub>2</sub><sup>VI</sup>Mo<sub>10</sub>V<sub>3</sub>O<sub>52</sub>·2H<sub>2</sub>O

(abbreviation: Se<sub>2</sub>Mo<sub>10</sub>V<sub>3</sub>), have not yet been studied. Here, we examined the anti-tumor effects of Se<sub>2</sub>Mo<sub>10</sub>V<sub>3</sub> and the mechanisms underlying those effects.

### RESULTS

#### Se<sub>2</sub>Mo<sub>10</sub>V<sub>3</sub> inhibited proliferation in K562 cells

As shown in Figure 1, Se<sub>2</sub>Mo<sub>10</sub>V<sub>3</sub> (12.5-100 mg/L) inhibited proliferation in K562 cells. The inhibitory rates for the 12.5, 25, 50, and 100 mg/L doses were 15.91±2.94, 16.64±0.97, 17.93±3.92, and 34.65±0.73% after 24 h (all *P*<0.05), 17.02±3.77, 20.78±0.15, 35.79±1.83, and 59.51±1.16% after 48 h (all *P*<0.05), and 30.12±3.76, 48.07±2.16, 62.93±1.63, and 92.77±1.51% after 72 h (all *P*<0.01), respectively, with IC<sub>50</sub> values of >100 mg/L after 24 h, 78.72±2.82 mg/L after 48 h, and 24.94±0.88

mg/L after 72 h. The inhibitory rate in control cells was set to 0. In positive control K562 cells treated with carboplatin (12.5-100 mg/L), IC<sub>50</sub> values were >100 mg/L after 24 h, 52.39 mg/L after 48 h, and 25.00 mg/L after 72 h. Similar inhibitory effects were observed in A549, CNE, SPCA-1, and Lewis cells after Se<sub>2</sub>Mo<sub>10</sub>V<sub>3</sub> treatment (data not shown).

### Se<sub>2</sub>Mo<sub>10</sub>V<sub>3</sub> induced apoptotic morphology in K562 cells

As shown in Figure 3, typical indicators of apoptosis, such as chromatin fragmentation, condensation and margination, cytoplasm vacuoles, and disappearance of cytolemma microvilli, were observed to a greater

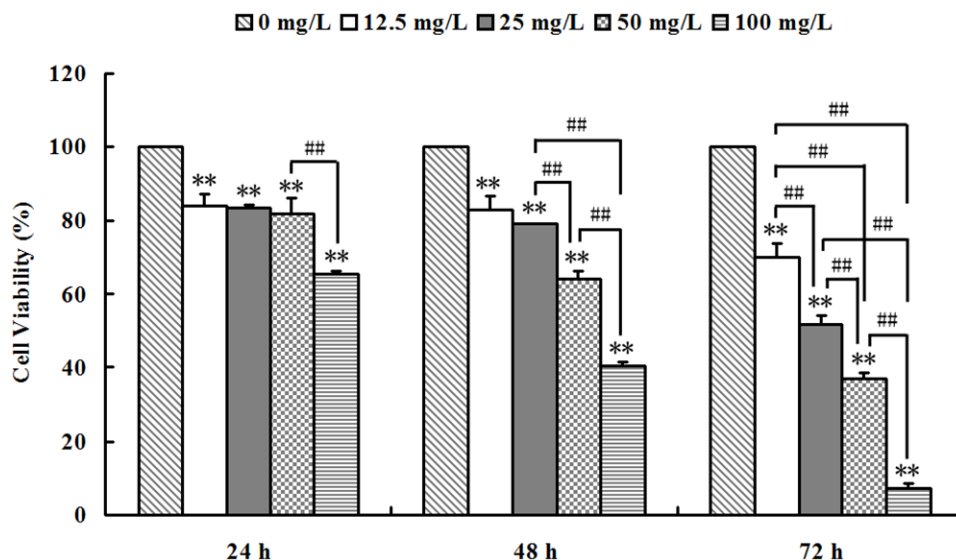


**Figure 1: Se<sub>2</sub>Mo<sub>10</sub>V<sub>3</sub> inhibited proliferation in K562 cells in an MTT assay.** Data are expressed as means ± S.D. of three independent experiments. \**P*<0.05, \*\**P*<0.01 versus control cells.

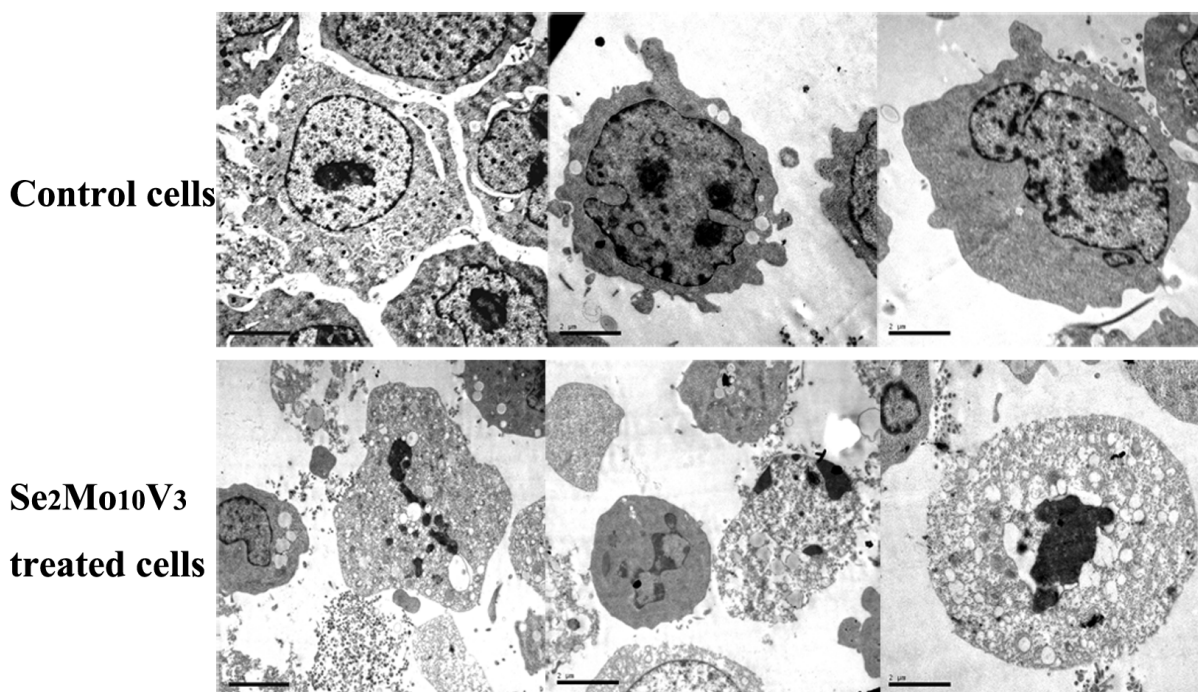


**Figure 2: 50 mg/L Se<sub>2</sub>Mo<sub>10</sub>V<sub>3</sub> induced apoptosis in K562 cells in a TEM experiment.** Scale = 2.00 μm. Data are representative of three independent experiments.

extent in K562 cells treated with 50 mg/L  $\text{Se}_2\text{Mo}_{10}\text{V}_3$  than in control cells, which were characterized by normal chromatin, uniform cytoplasm, the presence of cytolemma microvilli, and diastolic cell bodies.

### $\text{Se}_2\text{Mo}_{10}\text{V}_3$ increased $\text{Ca}^{2+}$ , $\text{Mg}^{2+}$ , $\text{H}^+$ , and ROS levels and decreased $\Delta\phi_m$ in K562 cells

The results of CLSM are shown in Figure 4. Intracellular  $\text{Ca}^{2+}$  levels increased after treatment with 25 or 50 mg/L  $\text{Se}_2\text{Mo}_{10}\text{V}_3$  (both  $P<0.05$ ). Intracellular  $\text{Mg}^{2+}$  levels also increased after treatment with 12.5, 25, or 50 mg/L  $\text{Se}_2\text{Mo}_{10}\text{V}_3$  (all  $P<0.01$ ). Intracellular  $\text{H}^+$  levels also increased, indicating that intracellular pH decreased, after treatment with 50 mg/L  $\text{Se}_2\text{Mo}_{10}\text{V}_3$  ( $P<0.05$ ). In addition, intracellular ROS levels increased after treatment with 12.5, 25, or 50 mg/L  $\text{Se}_2\text{Mo}_{10}\text{V}_3$  (all  $P<0.05$ ). Finally,  $\Delta\phi_m$  was markedly reduced after treatment with 50 mg/L  $\text{Se}_2\text{Mo}_{10}\text{V}_3$  ( $P<0.01$ ).

### $\text{Se}_2\text{Mo}_{10}\text{V}_3$ promoted cytoplasmic cytochrome C level, inhibited cytoplasmic $\text{I}\kappa\text{B}\alpha$ degradation and reduced nuclear NF- $\kappa\text{B}$ level in K562 cells

Western blotting results are shown in Figure 5. Cytoplasmic cytochrome C levels were increased in cells treated with 25, 50, or 100 mg/L  $\text{Se}_2\text{Mo}_{10}\text{V}_3$  (all  $P<0.01$ ), which indicated that the release of cytochrome C from the mitochondria into the cytoplasm was increased. Cytoplasmic  $\text{I}\kappa\text{B}\alpha$  degradations were decreased in cells treated with 50 or 100 mg/L, but not with 25 mg/L  $\text{Se}_2\text{Mo}_{10}\text{V}_3$  (both  $P<0.01$ ), and nuclear NF- $\kappa\text{B}$

levels were reduced in cells treated with 25, 50, or 100 mg/L  $\text{Se}_2\text{Mo}_{10}\text{V}_3$  (all  $P<0.01$ ), which indicated that the translocation of NF- $\kappa\text{B}$  from the cytoplasm to the nucleus was inhibited.

### $\text{Se}_2\text{Mo}_{10}\text{V}_3$ inhibited S180 and H22 cell growth *in vivo*

As shown in Figure 2, 5 or 10 mg/kg  $\text{Se}_2\text{Mo}_{10}\text{V}_3$  (i.g.) inhibited the growth of S180 cells by 35.6 and 39.4%, respectively (all  $P<0.01$ ). In S180 tumor-bearing mice, tumor weights were  $1.762\pm 0.642$ ,  $1.351\pm 0.442$ ,  $1.135\pm 0.275$ , and  $1.067\pm 0.379$  g after treatment with 0, 1, 5, and 10 mg/kg  $\text{Se}_2\text{Mo}_{10}\text{V}_3$ , respectively. Five or 10 mg/kg  $\text{Se}_2\text{Mo}_{10}\text{V}_3$  (i.g.) similarly inhibited the growth by 46.4 and 52.6%, respectively, in H22 cells (both  $P<0.05$ ). In H22 tumor-bearing mice, tumor weights were  $1.113\pm 0.447$ ,  $0.851\pm 0.203$ ,  $0.597\pm 0.212$ , and  $0.528\pm 0.351$  g after treatment with 0, 1, 5, and 10 mg/kg  $\text{Se}_2\text{Mo}_{10}\text{V}_3$ , respectively.

## DISCUSSION

In this study, we demonstrated that  $\text{Se}_2\text{Mo}_{10}\text{V}_3$ , a heteropoly compound containing selenium, had anti-tumor effects both *in vitro* and *in vivo*. Furthermore, we explored the mechanisms underlying its anti-tumor effects in K562 cells.

Apoptosis, a genetically controlled mechanism essential for the maintenance of tissue homeostasis and proper development, is crucial to the anti-tumor effects of many chemotherapeutics [9]. Here, we observed typical

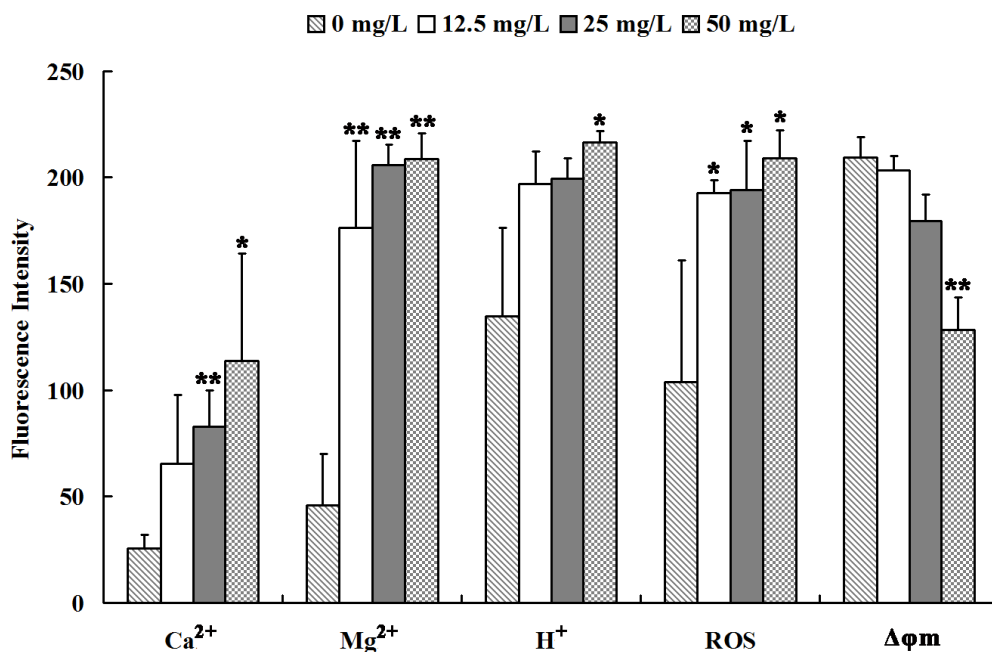


**Figure 3:**  $\text{Se}_2\text{Mo}_{10}\text{V}_3$  increased  $\text{Ca}^{2+}$ ,  $\text{Mg}^{2+}$ ,  $\text{H}^+$ , and ROS levels and decreased  $\Delta\phi_m$  in K562 cells in a CLSM experiment. Data are expressed as means  $\pm$  S.D. of three independent experiments. \* $P<0.05$ , \*\* $P<0.01$  versus control cells.

apoptotic morphology, including chromatin fragmentation, condensation and margination, cytoplasm vacuoles, and the absence of cytolemma microvilli, in  $\text{Se}_2\text{Mo}_{10}\text{V}_3$ -treated K562 cells here.  $\text{Ca}^{2+}$  and  $\text{Mg}^{2+}$  are key intracellular messengers that play important roles in the induction of apoptosis. Increases in cytosolic  $\text{Ca}^{2+}$  and  $\text{Mg}^{2+}$  levels have

been linked to the activation of a  $\text{Ca}^{2+}/\text{Mg}^{2+}$  dependent endonuclease which cleaves DNA to generate nucleosomal fragments (180-200 bp) during apoptosis [10, 11]. Here, we confirmed that  $\text{Se}_2\text{Mo}_{10}\text{V}_3$  increased intracellular  $\text{Ca}^{2+}$  and  $\text{Mg}^{2+}$  levels in K562 cells. Accumulating data also indicates that ROS have beneficial anti-cancer effects. For

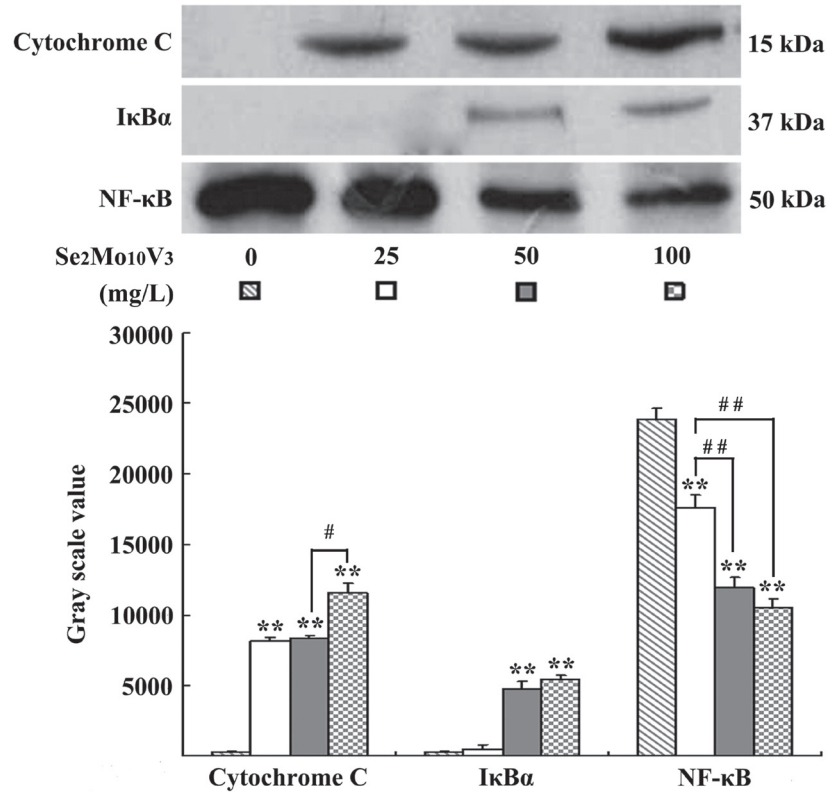


**Figure 4:  $\text{Se}_2\text{Mo}_{10}\text{V}_3$  promoted cytoplasmic cytochrome C level, inhibited cytoplasmic IκBα degradation and reduced nuclear NF-κB level in K562 cells in a Western blotting experiment.** Data are expressed as means ± S.D. of three independent experiments. \* $P < 0.05$ , \*\* $P < 0.01$  versus control cells.

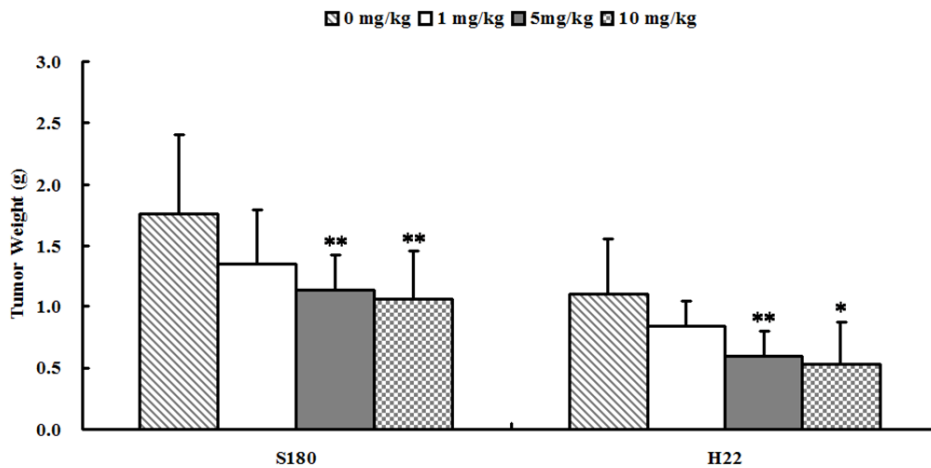


**Figure 5:  $\text{Se}_2\text{Mo}_{10}\text{V}_3$  inhibited the growth of S180 and H22 xenografts *in vivo*.** Data are expressed as means ± S.D. (n=10). \* $P < 0.05$ , \*\* $P < 0.01$  versus control tumor-bearing mice.



instance, increasing ROS levels can enhance apoptosis and thereby inhibit tumor growth [12]. Selenium can also induce the generation of ROS and apoptosis in tumor cells [13]. Moreover,  $\text{Na}_5\text{SeV}_5\text{O}_{18}\cdot\text{H}_{20}$ , an analog of  $\text{Se}_2\text{Mo}_{10}\text{V}_3$ , induced an increase in ROS levels in K562 cells [7]; here,  $\text{Se}_2\text{Mo}_{10}\text{V}_3$  also increased ROS levels in K562 cells. Efficient pH maintenance reduces apoptosis, suggesting that intracellular pH homeostasis and tumor development may be linked [14], and decreasing pH is a hallmark of apoptosis [7]. Consistent with these findings, we observed here that  $\text{Se}_2\text{Mo}_{10}\text{V}_3$  increased  $\text{H}^+$  levels, which corresponds to a decrease in pH, in K562 cells. During apoptosis, increasing mitochondrial permeability reduces  $\Delta\varphi_m$  and triggers release of cytochrome C into the cytoplasm [15]. Here,  $\text{Se}_2\text{Mo}_{10}\text{V}_3$  decreased  $\Delta\varphi_m$  and triggered the subsequent release of cytochrome C in K562 cells. Changes in the concentration of intracellular ions such as  $\text{Ca}^{2+}$  and  $\text{Mg}^{2+}$  may also induce mitochondrial impairment and reduce  $\Delta\varphi_m$  [16]. It is therefore possible that, in  $\text{Se}_2\text{Mo}_{10}\text{V}_3$ -treated K562 cells, decreased  $\Delta\varphi_m$  and cytochrome C release were triggered in part by increased levels of  $\text{Ca}^{2+}$  and  $\text{Mg}^{2+}$ . In conclusion, the results of this study together with previous findings indicate conclusively that  $\text{Se}_2\text{Mo}_{10}\text{V}_3$  induces the apoptosis of K562 cells.

To determine whether  $\text{Se}_2\text{Mo}_{10}\text{V}_3$ -induced apoptosis is mediated by the NF- $\kappa$ B/I $\kappa$ B $\alpha$  pathway, we also examined changes in NF- $\kappa$ B and I $\kappa$ B $\alpha$ . NF- $\kappa$ B translocation is normally inhibited by I $\kappa$ B proteins that sequester it in the cytoplasm after they are phosphorylated by I $\kappa$ B kinase. Degradation of I $\kappa$ B $\alpha$  thus allows nuclear translocation of NF- $\kappa$ B [17, 18]. It has been reported that NF- $\kappa$ B/I $\kappa$ B $\alpha$  is constitutively active in breast, colon, pancreatic, ovarian, lymphoma, and melanoma cancer cells. Furthermore, inhibition of this pathway using chemotherapeutics may be able to reverse or halt the growth and spreading of tumors [19]. Selenium compounds also inhibit NF- $\kappa$ B in tumor cells [17]. Here,  $\text{Se}_2\text{Mo}_{10}\text{V}_3$  inhibited the degradation of I $\kappa$ B $\alpha$  and the translocation of NF- $\kappa$ B in K562 cells. Shishodia and colleagues demonstrated that translocated NF- $\kappa$ B activates the expression of anti-apoptotic genes such as Bcl-2 and Bcl-xL, and the suppression of NF- $\kappa$ B inhibited the expression of these genes, thereby promoting apoptosis [20]. Immunocytochemistry also revealed that  $\text{Se}_2\text{Mo}_{10}\text{V}_3$  treatment decreased Bcl-2 expression and increased Bax expression in K562 (data not shown). An elevated Bax/Bcl-2 ratio increases spontaneous self-oligomerization of those molecules, which facilitates the reduction of  $\Delta\varphi_m$ , the release of cytochrome C into the cytoplasm, and, ultimately, apoptosis [21]. Based on these findings, it is likely that decreased  $\Delta\varphi_m$  and the release of cytochrome C in  $\text{Se}_2\text{Mo}_{10}\text{V}_3$ -treated K562 cells are triggered in part by an elevated Bax/Bcl-2 ratio.

In summary,  $\text{Se}_2\text{Mo}_{10}\text{V}_3$  inhibits tumor growth both *in vitro* and *in vivo* and induces apoptosis in K562 cells at least in part by inhibiting NF- $\kappa$ B/I $\kappa$ B $\alpha$ . Our results indicate that  $\text{Se}_2\text{Mo}_{10}\text{V}_3$  may be a useful component of

clinical therapy. Further research is needed to examine the anti-leukocythemia effects of  $\text{Se}_2\text{Mo}_{10}\text{V}_3$  *in vivo* and to evaluate its preclinical safety on animals.

## MATERIALS AND METHODS

### Drugs and chemicals

$\text{Se}_2\text{Mo}_{10}\text{V}_3$  (yellow crystal, purity >99%) was synthesized by the State Key Laboratory of Applied Organic Chemistry, Lanzhou University, China. Briefly, solution 1 (0.29 g  $\text{NH}_4\text{VO}_3$  dissolved in 10 mL hot water) and solution 2 (1.85 g  $(\text{NH}_4)_6\text{Mo}_7\text{O}_{24}\cdot 4\text{H}_2\text{O}$  dissolved in 8 mL hot water) were blended and 0.063 g/mL  $\text{Na}_2\text{SeO}_4$  were added while stirring (solution 3). Solution 3 was adjusted to a pH of 2 using  $\text{H}_2\text{SO}_4$  (1:1), and its color changed from orange red to crimson (solution 4). Solution 4 was stirred with reflux at 90°C for 10 h (solution 5). Solution 5 was filtered while hot. The filtrate was placed at room temperature and the yellow crystals separated out quickly. After vacuum filtration, the crystal was washed using an aqueous solution (pH was adjusted to 2 using  $\text{H}_2\text{SO}_4$  (1:1)) and dried. The weight of the crude product was 0.68g. The crude product was recrystallized 2 times using an aqueous solution (pH=2). 1.12g yellow crystal was obtained ( $\text{Se}_2\text{Mo}_{10}\text{V}_3$ ). The yellow crystal decomposed readily in the air and was slightly soluble in water, methanol, DMSO, and acetone [22]. RPMI-1640 nutrient solution was purchased from Invitrogen. Fetal bovine serum was purchased from Sijiqing Co. 3-(4,5-dimethylthiazol-2-yl)-2,5-diphenyl tetrazolium bromide (MTT) was purchased from Sigma.

### Cell culture

The human chronic myelogenous leukemia K562 cell line was supplied by Shanghai Cell Bank, Chinese Academy of Sciences and grown in RPMI-1640 nutrient solution supplemented with 10% fetal bovine serum, 2 mM L-glutamine, 100 units/mL penicillin, and 100  $\mu$ g/mL streptomycin in a humidified 5%  $\text{CO}_2$  incubator at 37°C. The *in vitro* experiments were performed using a concentration of  $1\times 10^5$  cells/mL.

### MTT assay

Cytotoxicity was measured in an MTT assay with slight modifications. K562 cells were treated with 12.5, 25, 50, or 100 mg/L  $\text{Se}_2\text{Mo}_{10}\text{V}_3$  for 24, 48, or 72 h. MTT solution was then added and the cells were incubated for an additional 4 h. The formazan crystals were dissolved with SDS solution and quantified using a microplate reader (ELx800, Bio-TEK). Cytotoxicity is presented as percent inhibition relative to the control cells. The half-maximal inhibitory concentrations (IC50) for  $\text{Se}_2\text{Mo}_{10}\text{V}_3$  in K562 cells were calculated using IC50 calculation software.

## Transmission electron microscopy (TEM)

K562 cell morphology was examined using TEM. Cells were treated with 50 mg/L  $\text{Se}_2\text{Mo}_{10}\text{V}_3$  for 24 h. Cell precipitates were then fixed with glutaraldehyde, post-fixed with osmium tetroxide, dehydrated with a graded alcohol series, immersed in epoxy resin and acetone, and embedded in epoxy resin. Ultra-thin sections were then prepared, dyed using uranyl acetate and lead citrate, and examined with a JEM-100 CX-II TEM (Jeol).

## Confocal laser scanning microscopy (CLSM)

Levels of  $\text{Ca}^{2+}$ ,  $\text{Mg}^{2+}$ ,  $\text{H}^+$ , and reactive oxygen species (ROS) and mitochondrial membrane potential ( $\Delta\varphi_m$ ) in K562 cells were determined by CLSM. Cells were treated with 12.5, 25, or 50 mg/L  $\text{Se}_2\text{Mo}_{10}\text{V}_3$  for 24 h. The cells were then incubated with Fluo-3/AM (5  $\mu\text{mol/L}$ ), Mag-fluo-4 (5 mmol/L), Carboxy SNARF-1/AM (10  $\mu\text{mol/L}$ ), 2',7'-dichlorofluorescein diacetate D-399 (5  $\mu\text{g/mL}$ ), and Mito Tracker Green FM (1.25  $\mu\text{mol/L}$ ) (Molecular Probes, OR, USA) for 30-45 min at 37°C to determine the intracellular  $\text{Ca}^{2+}$ ,  $\text{Mg}^{2+}$ ,  $\text{H}^+$ , and ROS levels and  $\Delta\varphi_m$ , respectively. Cells were then washed with RPMI-1640 medium and examined under a TCS SP2 CLSM (Leica, Germany). The results were analyzed with Leica Confocal software.

## Western blotting

Cytochrome C, I $\kappa$ B $\alpha$ , and NF- $\kappa$ B in K562 cells were detected by Western blotting. Cells were treated with 25, 50, or 100 mg/L  $\text{Se}_2\text{Mo}_{10}\text{V}_3$  for 24 h, resuspended in buffer A (10 mM Hepes-NaOH (pH 7.8), 15 mM KCl, 1 mM  $\text{MgCl}_2$ , 0.1 mM EDTA, 1 mM DTT, 1 mM PMSF, 1 mg/L Leupeptin, and 1% NP-40), and incubated on ice for 30 min. The samples were then centrifuged at 12,000  $\times$ g for 30 min at 4°C and the supernatants were used as cytoplasmic extracts. The remaining pellets were resuspended in buffer B (20 mM Hepes-NaOH (pH 7.9), 1.5 mM  $\text{MgCl}_2$ , 0.42 M NaCl, 0.2 mM EDTA, 25% glycerol, 0.5 mM DTT, 0.5 mM PMSF, and 1 mg/L Leupeptin), incubated on ice for 30 min, and centrifuged at 14,000  $\times$ g for 30 min at 4°C. The supernatants were used as nuclear extracts. All supernatants were quantified and run on 12% or 15% SDS polyacrylamide gels. Separated proteins were transferred from the gels to nitrocellulose membranes. The remaining procedures were performed according to the instructions provided with the LumiGLO Western blotting kit (KPL, MD, USA). Mouse monoclonal anti-cytochrome C (1:1000) (Invitrogen, CA, USA), rabbit monoclonal anti-I $\kappa$ B $\alpha$  (1:1000) (Abcam, MA, USA), and rabbit monoclonal anti-NF- $\kappa$ B (1:250) (Zymed Laboratory, CA, USA) were used as primary antibodies. Immunoblotting results were semi-quantified using Quantity One software (Bio-Rad).

## Animals and xenograft tumor experiments

5-week old female mice (species: Kun-Ming; strain: Swiss) weighing 20.0 $\pm$ 2.0 g were purchased from the GLP Laboratory, Lanzhou University (Grade II, Certificate No. 14-005). They were housed at 23 $\pm$ 1 °C under 12h light/12h dark conditions with *ad libitum* access to food and water. All animal experiments were performed in accordance with relevant guidelines and regulations approved by the Experimental Animal Research Committee of Lanzhou University. According to standard xenograft tumor research protocols, mice were given subcutaneous injections of 3 $\times$ 10<sup>6</sup> sarcoma 180 (S180) or hepatoma 22 (H22) cells in the exponential growth phase into the right axillary fossa on day 0. On day 1, mice were randomly divided into control, low, middle, and high dose groups and were treated daily with 0.9% normal saline or 1, 5, or 10 mg/kg  $\text{Se}_2\text{Mo}_{10}\text{V}_3$ , i.g., respectively (n=10 per group). The mice were sacrificed on day 10 and the tumors were removed and weighed. Inhibition of tumor growth was evaluated using percent inhibition relative to tumor weights in control tumor-bearing mice.

## Statistical analysis

Data are shown as means  $\pm$  S.D. of three independent experiments. Statistical analysis were performed using one-way ANOVA and the LSD method in SPSS 22.0 software. Differences were considered statistically significant when  $P < 0.05$ .

## Abbreviations

$\text{Se}_2\text{Mo}_{10}\text{V}_3$ ,  $(\text{NH}_4)_2\text{H}_{15}\text{Se}_2\text{Mo}_{10}\text{V}_3\text{O}_{52}\cdot 2\text{H}_2\text{O}$ . IC50, half-maximal inhibitory concentration. TEM, transmission electron microscope.  $\Delta\varphi_m$ , mitochondrial membrane potential. CLSM, confocal laser scanning microscopy. S180, sarcoma 180. H22, hepatoma 22.

## Author contributions

H.-N. Z. performed the experiments. W.-L. F. helped to perform the *in vitro* experiment. C.-N. A. wrote the manuscript, prepared the figures and supplied important supports. W.-G. L. designed the project. All authors reviewed the manuscript.

## CONFLICTS OF INTEREST

The authors declare no conflicts of interest.

## FUNDING

This work was supported by the Natural Science Foundation of Gansu Province, China (ZS001-A23-059Y).

## REFERENCES

1. Alfthan G, Euroala M, Ekholm P, Venäläinen ER, Root T, Korkalainen K, Hartikainen H, Salminen P, Hietaniemi V, Aspila P, Aro A. Effects of nationwide addition of selenium to fertilizers on foods, and animal and human health in Finland: from deficiency to optimal selenium status of the population. *J Trace Elem Med Bio*. 2015; 31: 142-147.
2. Navarro-Alarcon M, Cabrera-Vique C. Selenium in food and the human body: a review. *Sci Total Environ*. 2008; 400: 115-141.
3. Klein EA. Selenium: epidemiology and basic science. *J Urol*. 2004; 171: S50-S53.
4. Endo M, Hasegawa H, Kaneko T, Kanno C, Monma T, Kano M, Shinohara F, Takahashi T. Antitumor activity of selenium compounds and its underlying mechanism in human oral squamous cell carcinoma cells: a preliminary study. *J Oral Maxil Surg*. 2017; 29: 17-23.
5. de Miranda JX, Andrade Fde O, Conti AD, Dagli ML, Moreno FS, Ong TP. Effects of selenium compounds on proliferation and epigenetic marks of breast cancer cells. *J Trace Elem Med Biol*. 2014; 28: 486-491.
6. Zeng HW, Combs GF Jr. Selenium as an anticancer nutrient: roles in cell proliferation and tumor cell invasion. *J Nutr Biochem*. 2008; 19: 1-7.
7. Yang JY, Wang ZR. The antitumor effects of selenium compound  $\text{Na}_3\text{SeV}_5\text{O}_{18}\cdot 3\text{H}_2\text{O}$  in K562 cell. *Arch Pharm Res*. 2006; 29: 859-865.
8. Fernandes AP, Gandin V. Selenium compounds as therapeutic agents in cancer. *Biochim Biophys Acta* 2015; 1850: 1642-1660.
9. Vázquez R, Riveiro ME, Vermeulen M, Mondillo C, Coombes PH, Crouch NR, Ismail F, Mulholland DA, Baldi A, Shayo C, Davio C. Toddaculin, a natural coumarin from *Toddalia asiatica*, induces differentiation and apoptosis in U-937 leukemic cells. *Phytomedicine*. 2012; 19: 737-746.
10. McConkey DJ, Orrenius S. The role of calcium in the regulation of apoptosis. *J Leukocyte Biol*. 1996; 59: 775-783.
11. Cain K, Inayat-Hussain SH, Kokileva L, Cohen GM. DNA cleavage in rat liver nuclei activated by  $\text{Mg}^{2+}$  or  $\text{Ca}^{2+} + \text{Mg}^{2+}$  is inhibited by a variety of structurally unrelated inhibitors. *Biochem Cell Biol*. 1994; 72: 631-638.
12. Salganik RI. The benefits and hazards of antioxidants: controlling apoptosis and other protective mechanisms in cancer patients and the human population. *J Am Coll Nutr*. 2001; 20: 464S-472S.
13. Jung U, Zheng X, Yoon SO, Chung AS. Se-methylselenocysteine induces apoptosis mediated by reactive oxygen species in HL-60 cells. *Free Radic Bio Med*. 2001; 31: 479-489.
14. Wenzel U, Daniel H. Early and late apoptosis events in human transformed and non-transformed colonocytes are independent on intracellular acidification. *Cell Physiol Biochem*. 2004; 14: 65-76.
15. Iannolo G, Conticello C, Memeo L, De Maria R. Apoptosis in normal and cancer stem cells. *Crit Rev Oncol Hematol*. 2008; 66: 42-51.
16. Bolduc JS, Denizeau F, Jumarie C. Cadmium-induced mitochondrial membrane-potential dissipation does not necessarily require cytosolic oxidative stress: studies using rhodamine-123 fluorescence unquenching. *Toxicol Sci*. 2004; 77: 299-306.
17. Gasparian AV, Yao YJ, Lü J, Yemelyanov AY, Lyakh LA, Slaga TJ, Budunova IV. Selenium compounds inhibit I $\kappa$ B kinase (IKK) and nuclear factor- $\kappa$ B (NF- $\kappa$ B) in prostate cancer cells. *Mol Cancer Ther*. 2002; 1: 1079-1087.
18. Wu H, Jiang K, Yin N, Ma X, Zhao G, Qiu C, Deng G. Thymol mitigates lipopolysaccharide-induced endometritis by regulating the TLR4- and ROS-mediated NF- $\kappa$ B signaling pathways. *Oncotarget*. 2017; 8: 20042-20055. doi: 10.18632/oncotarget.15373.
19. Miller SC, Huang R, Sakamuru S, Shukla SJ, Attene-Ramos MS, Shinn P, Van Leer D, Leister W, Austin CP, Xia M. Identification of known drugs that act as inhibitors of NF- $\kappa$ B signaling and their mechanism of action. *Biochem Pharmacol*. 2010; 79: 1272-1280.
20. Shishodia S, Amin HM, Lai R, Aggarwal BB. Curcumin (diferuloylmethane) inhibits constitutive NF- $\kappa$ B activation, induces G1/S arrest, suppresses proliferation, and induces apoptosis in mantle cell lymphoma. *Biochem Pharmacol*. 2005; 70: 700-713.
21. Rudner J, Elsaesser SJ, Müller AC, Belka C, Jendrossek V. Differential effects of anti-apoptotic Bcl-2 family members Mcl-1, Bcl-2, and Bcl-xL on Celecoxib-induced apoptosis. *Biochem Pharmacol*. 2010; 79: 10-20.
22. Ju ZH, Wu JG. Studies on some heteropoly compounds containing selenium 68-75 (Graduate Dissertation Library of Lanzhou University, 2004).